Mosher, D.C., Erbacher, J., and Malone, M.J. (Eds.)
Proceedings of the Ocean Drilling Program, Scientific Results Volume 207

1. Leg 207 Synthesis: Extreme Warmth, Organic-Rich Sediments, and an Active Deep Biosphere: Cretaceous–Paleogene Paleoceanographic Depth Transect at Demerara Rise, Western Tropical Atlantic[1]

David C. Mosher,[2] Jochen Erbacher,[3] and Mitch Malone[4]

ABSTRACT

Rapid and extreme perturbations of climate and the global carbon cycle occurred during the Cretaceous and Paleogene periods. Demerara Rise, a submarine plateau in the western equatorial Atlantic Ocean, is ideally located and hosts the sedimentary sequences to sample and investigate these events. Ocean Drilling Program (ODP) Leg 207 was designed to core a depth transect of these sediments on the outer flank of Demerara Rise, spanning modern water depths of 1900–3200 m. During the leg, near-continuous records of Late Cretaceous and Paleogene sedimentary successions from this locale were successfully recovered, including the mid-Cenomanian ocean anoxic event (MCE), Late Cretaceous ocean anoxic event (OAE 2), Cretaceous/Paleogene (K/P) boundary event, and Paleocene/Eocene Thermal Maximum (PETM).

The sampled stratigraphy is dominated by two lithologic components: terrigenous detritus and biogenic carbonate and silica. This stratigraphy is broadly categorized into three main styles of deposition: (1) synrift/syntransform clastics, (2) restricted marine "black shales," and (3) open marine chalks and calcareous claystones. Strong physical property contrasts in each of these litho-types allows for excellent core to seismic reflection profile correlation. High-quality seismic reflection data through each drill site permits excellent linkage between drill sites.

[1]Mosher, D.C., Erbacher, J., and Malone, M.J., 2007. Leg 207 synthesis: extreme warmth, organic-rich sediments, and an active deep biosphere, Cretaceous–Paleogene paleoceanographic depth transect at Demerara Rise, western tropical Atlantic. *In* Mosher, D.C., Erbacher, J., and Malone, M.J. (Eds.), *Proc. ODP, Sci. Results,* 207: College Station, TX (Ocean Drilling Program), 1–26. doi:10.2973/odp.proc.sr.207.101.2007
[2]Natural Resources Canada, Geological Survey of Canada–Atlantic, Bedford Institute of Oceanography, 1 Challenger Drive, PO Box 1002, Dartmouth NS, Canada.
dmosher@nrcan.gc.ca
[3]Bundesanstalt für Geowissenschaften und Rohstoffe, Postfach 51 01 53, Alfred-Benz-Haus, Stilleweg, 30641 Hanover, Germany.
[4]Integrated Ocean Drilling Program, Texas A&M University, 1000 Discovery Drive, College Station TX 77845-9541, USA.

Initial receipt: 9 June 2006
Acceptance: 6 March 2007
Web publication: 20 April 2007
Ms 207SR-101

Oldest sediments recovered during Leg 207 are late Albian in age, and marine conditions are suggested by their composition. A major regional unconformity tops these sediments, leading into organic-rich, laminated claystones (black shales) indicative of oxygen depletion within a restricted basin. The onset of black shale deposition was transgressive from the latest Albian to latest Cenomanian and coincided with transform margin separation of South America and Africa. Carbon and oxygen isotope studies indicate bottom water temperatures were warm through the Cenomanian, and a pronounced $\delta^{13}C$ excursion in the mid-Cenomanian reflects the MCE. During the late Cenomanian, $\delta^{18}O$ isotope values and TEX_{86} biomarker data indicate warm surface waters and decreased salinity suggesting restricted ocean circulation conditions at Demerara Rise. Positive carbon isotope values, high total organic carbon contents, elevated Fe/Al and Co/Al ratios, and lack of benthic foraminifers indicate severe anoxia and an increase in surface water productivity during OAE 2, a global ocean oxygen depletion event. The Late Cretaceous saw a return of salinity conditions and gradual sea-surface water temperature cooling. Reoxygenation gradually occurred during the Santonian, and black shale deposition ceased on Demerara Rise in the early Campanian. Chalk and calcareous claystone deposition followed through the late Campanian–Maastrichtian interval.

The organic matter of the Cretaceous black shale sequence is dominantly marine in origin. Although results of microbial observations through this interval are inconclusive, geochemical data (e.g., linear gradients of ammonium and sulfate from the top of the black shales to the seafloor and trace metal anomalies) indicate that these sediments are active bioreactors dominating the pore water chemistry.

At three of the Leg 207 drill sites (1258, 1259, and 1260) excellent examples of the Cretaceous/Paleogene boundary were recovered, marked by a 2-cm-thick graded spherule layer and a spike in iridium concentration. This layer resulted from atmospheric fallout from the proposed Chicxulub meteorite impact. Faunal turnover at this boundary is dramatic. The Paleocene/Eocene boundary event was recovered at all five sites, marked again by faunal turnover and a significant drop in carbon isotope values as well as a change in sediment texture and color.

The Eocene sedimentary succession is well represented in Leg 207 cores. $\delta^{13}C$ and $\delta^{18}O$ data from benthic foraminifers reveal a general middle Eocene cooling with short-lived warming events that were previously unrecognized. A regional mid- or late Miocene erosional event, possibly brought on by marked changes in global ocean circulation, sporadically removes much of the upper Eocene and lower Neogene succession on the outer Demerara Rise. The locale is largely sediment-starved at this time, with only a thin Quaternary sediment cover.

INTRODUCTION

Spectacular examples of rapid (1 k.y. to 1 m.y.) perturbations of the global carbon cycle and extreme changes in Earth's climate occurred during the Cretaceous and Paleogene periods (e.g., Cretaceous oceanic anoxic events [OAEs] and the Paleocene/Eocene Thermal Maximum [PETM]) (Erbacher et al., 2003; Zachos et al., 2001, 2006; Wilson et al., 2002). In many cases, these events were accompanied by widespread extinction of marine and terrestrial biota (e.g., Coxall et al., 2006). Many questions remain, however, about the underlying causes and effects of

these critical events in Earth history. High-resolution paleoceanographic records from ocean drill sites, particularly from tropical regions that are important in driving global ocean-atmospheric circulation, help address these gaps in understanding.

Demerara Rise is a submarine plateau that is an apparent extension of the continental margin north of Suriname and French Guyana, South America, located in the tropics just north of the Equator between 8° and 10°N latitude and 52° and 56°W longitude (Fig. F1). The rise stretches ~380 km along the South American coast and is ~220 km wide from the shelf break to the northeastern escarpment, where water depths increase from 1000 to >4500 m (Fig. F1). Its geographic and tectonic position makes it an ideal location to investigate late-stage Atlantic rifting and opening of the Atlantic Gateway in the mid- to Late Cretaceous. The outer Demerara Rise is known to contain shallowly buried and expanded sections of Cretaceous- and Paleogene-age sediments (Hayes, Pimm, et al., 1972; Erbacher, Mosher, Malone, et al., 2004). Ocean Drilling Program (ODP) Leg 207 focused on sampling these Cretaceous and Paleogene deep-sea sediments at the northwestern extent of the rise (~9°N, in 1800–3400 m water depth) (Fig. F1). During the leg, continuous records of the PETM, Cretaceous/Paleogene (K/P) boundary, and OAEs were successfully recovered.

F1. Location map of outer Demerara Rise, p. 16.

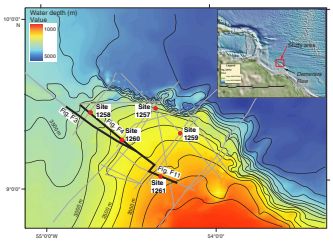

RATIONALE

The ODP program planning group (PPG) Extreme Climates of the Paleogene and Cretaceous was established to foster new drilling proposals for studying the greenhouse climate and extreme events during the Cretaceous–Paleogene. A group of scientists from this PPG designed Leg 207, the primary objective of which was to recover shallowly buried and relatively expanded Cretaceous–Paleogene sediments along a paleodepth transect in the tropical Atlantic to obtain sample material for paleoceanographic reconstructions. The second important objective of Leg 207 was to recover organic matter–rich sediments, which were expected to provide a great potential to serve as substrates for an active microbial population. Precruise plans were to perform extensive advanced piston coring (APC) on multiple overlapping holes at each site in order to recover complete stratigraphic sections. Unexpected stiffness of Eocene–Cretaceous sediments, however, forced the use of rotary core barrel (RCB) drilling for this interval. This modified drilling strategy yielded approximately 75% recovery of core material and was successful enough to construct spliced sections of several stratigraphic intervals for 13 holes at 5 sites (Sites 1257–1261). Multiple coring of the Cretaceous–Paleogene chalks, claystones, and black shales recovered a number of critical time slices and events such as the late Albian OAE 1d, the mid-Cenomanian Event (MCE), the late Cenomanian OAE 2, the Santonian OAE 3, the opening of the equatorial Atlantic in the Santonian–early Campanian, the K/P boundary, and the PETM (Erbacher et al., 2004; Erbacher, Mosher, Malone, et al., 2004). Correlative sequences from different paleowater depths were recovered for many of these events, allowing study of the vertical structure of the Atlantic Ocean during these intervals.

STRUCTURAL EVOLUTION AND STRATIGRAPHIC SUMMARY

Demerara Rise is a promontory of the South American continental crust that is conjugate to the Guinea Plateau of west Africa (Fig. F2). The northern margin of Demerara Rise is bounded by a transform fracture system that extends fully eastward to the coast of West Africa, north of which is the Guinea Plateau (Fig. F2). In the Late Jurassic, Demerara Rise and the Guinea Plateau formed the southern margin of the North Atlantic Ocean. At that time, Demerara Rise was likely a marginal sea in which evaporites and shallow-water carbonates formed (Gouyet et al., 1994; Benkhelil et al., 1995). By the Early Cretaceous, mid-Atlantic Ridge extension, rifting, and dextral transform shear motion separated the two plateaus. Following initial rifting and transform motion, subsidence was presumably rapid throughout the Early and mid-Cretaceous as a result of thermal cooling (Flicoteaux et al., 1988). Additionally, global sea level continued to rise rapidly through this period (Haq et al., 1988). This subsidence and sea level rise created accommodation space for thick sediment accumulation on this portion of the continental margin. These sediments have been imaged with industry multichannel seismic (MCS) data but were not sampled during Leg 207 (Fig. F3). The overlying postrift upper Mesozoic and Cenozoic sediments were best imaged with site survey high-resolution MCS reflection data (e.g., Fig. F4), however, and were sampled at the five Leg 207 drill sites (Fig. F1).

The most distinctive seismic reflection event apparent on all seismic profiles imaged from outer Demerara Rise is a regionally correlative horizon, designated "C" (Fig. F3). Reflections overlying the C horizon appear largely conformable. Underlying reflections truncate upward against the C surface, forming an angular unconformity. This underlying section consists of pre-Albian synrift and syntransform sediments. High-amplitude reflectors are more or less continuous and parallel, although tilted and locally divergent. Near-vertical strike-slip faults and a near-vertical outer (eastern) margin of Demerara Rise are evidence of transform tectonics. Apparent normal listric faults are probably representative of margin subsidence. The C horizon is referred to as a "breakup" unconformity, likely representing the final separation of Demerara Rise and the Guinea Plateau concurrent with opening of the Atlantic Gateway.

The principal stratigraphic section of interest for Leg 207 was the interval above the C horizon, which is largely Late Cretaceous and Paleogene in age. Four regionally correlated reflection events within this section provided the seismic stratigraphic framework for the Leg 207 drilling program (Fig. F4). These events were correlated with drilling results through generation of synthetic seismograms (Fig. F5). Above the C surface is a ~70- to 100-ms-thick sequence of medium-amplitude, parallel, largely flat lying coherent reflections. This sequence corresponds to Cenomanian–Turonian organic-rich claystone observed at the drill sites (lithologic Unit IV of Erbacher, Mosher, Malone, et al., 2004). At the top of this seismic sequence is a reflection event (B′) that corresponds to the top of the black shale sequence. A ~50-ms-thick sequence above B′ and below Reflector B typically shows lower amplitude but conformable reflections corresponding to the Campanian–Maastrictian section of nannofossil chalk to calcareous silt and claystone (lithologic Subunit IIIB) observed during Leg 207. O'Regan and Moran (this vol-

F2. Demerara Rise and Guinea Plateau separated by the Guinea Fracture Zone, p. 17.

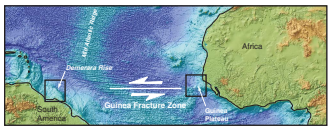

F3. MCS line showing the C reflector and pattern of subsurface faulting, p. 18.

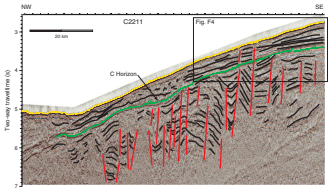

F4. Seismic stratigraphy above the C reflection horizon, p. 19.

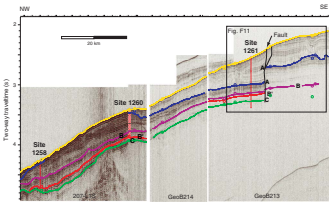

F5. Seismic to core correlation conducted with a synthetic seismogram, p. 20.

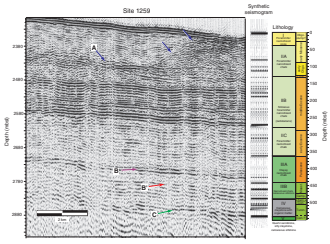

ume) found significant physical property differences including a marked reduction in permeability in the transition between the lithologies of Units IV and III, explaining the distinctive seismic signatures each produces and the good correlations of seismic to core data. The high-amplitude B reflector at the top of lithologic Subunit IIIB ties to the K/P boundary, shown particularly well with core-seismic correlations at three of the Leg 207 sites (1259, 1260, and 1261).

Between the B reflector and the overlying A horizon is a variably thick unit largely composed of parallel, coherent, flat-lying reflections that correlates with a Paleogene sequence of foraminifer nannofossil chalk to clayey nannofossil chalk (lithologic Subunits IIIA, IIC, and IIB) (Fig. F5). The A horizon is an erosional surface of probable Miocene age (it was not specifically sampled during drilling) that apparently resulted in significant removal of section on the outer flank, leaving mostly Paleocene and lower to middle Eocene sediments. This latter section thins toward the north and toward the flanks of the rise. The Neogene section above the A surface is nearly absent on the outermost portions of Demerara Rise but thickens inboard. It consists of nannofossil clay (lithologic Unit I) and is >300 m thick at Site 1261.

Hetzel et al. (this volume) produced quantitative geochemical characterization of the five lithologic units using bulk total inorganic carbon, total organic carbon, sulfide, a suite of major and minor elements, and rare earth elements. They divided the Leg 207 lithostratigraphy into three depositional modes: synrift clastics (Unit V), laminated black shales (Unit IV), and open-marine chalk and calcareous claystones (Units III, II, and I). Their results indicate that major element compositions are dominated by a mixture of two components: terrigenous detritus and biogenic carbonate and silica. The terrigenous component in most of the sedimentary section has the composition of average shale. In contrast, Unit I is composed of a more clay dominated weathered terrigenous component. The Cretaceous black shales of Unit IV are enriched in redox-sensitive and stable sulfide elements (Mo, V, Zn, and As). Combined with high phosphate contents and a pronounced Ce anomaly, these data confirm high paleoproductivity and oxygen depletion in the water column during deposition of Unit IV.

Late Albian to Early Campanian Paleoceanography

Oldest sediments recovered during Leg 207 are lower upper Albian claystones and silty claystones. These claystones are rich in organic matter and phosphatic concretions at Site 1258 and contain less organic matter at Sites 1257 and 1260. A dominance of marine organic matter as well as the presence of fossils indicating normal open-marine conditions (e.g., ammonites, calcareous nannofossils, and foraminifers) demonstrate that the distal parts of Demerara Rise were occupied by an open-marine and epicontinental basin (Meyers et al., 2006; **Meyers and Bernasconi,** this volume; Owen and Mutterlose, 2006; Kulhanek and Wise, 2006). Lower upper Albian claystones are unconformably overlain by organic-rich, laminated black shales. At the deepest site (Site 1258), these black shales are latest Albian in age (Kulhanek and Wise, 2006), potentially representing OAE 1d.

The hiatus between lower upper Albian claystones and uppermost Albian black shales, recognized as the C horizon on seismic data, dates an important stage in the evolution of the continental margin from the rift to drift stage and from sedimentation in an epicontinental basin to open oceanic conditions. **O'Regan** (this volume) used log and core

physical property data from multiple holes at each drill site to generate composite stratigraphic depth scales (in units of equivalent log depth [eld]) for the black shale interval. The onset of black shale deposition is transgressive, starting in the latest Albian at Site 1258, the early Cenomanian at Sites 1260 and 1257, the late Cenomanian at Site 1261, and the latest Cenomanian at Site 1259 (Erbacher et al., 2005). These results indicate establishment of an apparently stable and long-lasting oxygen minimum zone at Demerara Rise.

Cenomanian Black Shales and the Mid-Cenomanian Event

Several chemical indicators suggest severe dysoxia to even anoxic conditions during the Cenomanian–Santonian at Demerara Rise. **Böttcher et al.** (this volume) compared conditions on Demerara Rise with those from the present-day Black Sea, as the abundance of reactive iron indicates anoxic conditions in the water column and within the sediment. Their observation is supported by high C/N ratios and low nitrogen isotope values, which might be the result of depressed organic matter degradation and microbial nitrogen fixation in an anoxic water column (Meyers et al., 2006). Benthic foraminifers, however, were observed throughout the black shale interval, arguing for frequent reoxygenation of the seafloor (Friedrich et al., 2006).

Low-resolution stable oxygen isotope data from Norris et al. (2002), Bornemann and Norris (in press), and Bice et al. (2006), as well as high-resolution data from Friedrich et al. (2006) and Moriya et al. (in press), demonstrated that sea-surface temperatures (SSTs) and bottom water temperatures at Demerara Rise were warm throughout the Cenomanian. Stable carbon isotopes from foraminiferal calcite and bulk organic matter record a pronounced positive excursion in the mid-Cenomanian that represents the mid-Cenomanian Event (MCE). At Demerara Rise, the MCE marks a major turnover in calcareous nannofloras (Hardas and Mutterlose., 2006) and benthic foraminifers (Friedrich et al., 2006). Above the MCE, $\delta^{18}O$ values of benthic foraminifers increase, suggesting either a pronounced cooling of bottom waters or a significant influence of saline waters at the seafloor (Friedrich et al., 2006). Cyclic sediment composition variations through this interval are inferred to represent eccentricity and precession cycles (**Nederbragt et al.,** this volume).

Although benthic foraminiferal assemblages document oxygen-poor conditions at the seafloor throughout the Cenomanian, above the MCE oxygen seems to have been even more deficient (Friedrich et al., 2006). Friedrich et al. (2006) favor a model where warm arid conditions during the late Cenomanian led to increased evaporation in tropical epicontinental basins such as the La Luna Sea west and southwest of Demerara Rise that served as sources of saline deep or intermediate waters that bathe Demerara Rise. $\delta^{18}O$ values of benthic foraminifers decrease in the uppermost Cenomanian at the base of OAE 2, which is interpreted as a decrease of bottom water salinity associated with a shutdown of deepwater production in tropical epicontinental basins, probably due to an increase of precipitation associated with OAE 2.

Oceanic Anoxic Event 2

Arguably, the most prominent and widespread of the mid-Cretaceous oceanic anoxic events is OAE 2 near the Cenomanian/Turonian bound-

ary. The isotope excursion as well as the distribution of organic-rich sediments is truly global, and both have been described from numerous outcrops and deep-sea cores around the world (for example, see **Nederbragt et al.,** this volume). At Demerara Rise, a pronounced positive carbon isotope excursion of as much as 6.5‰, during OAE 2, was recorded by Erbacher et al. (2005) (Fig. **F6**). Rather complete OAE 2 successions are preserved at Sites 1258, 1260, and 1261. High-resolution carbon isotope and calcareous nannoplankton stratigraphies across the OAE enabled a detailed correlation of the Leg 207 sites with sections elsewhere in the world (Erbacher et al., 2005; Hardas and Mutterlose, 2006; **Nederbragt et al.,** this volume).

Late Cenomanian surface water temperatures at Demerara Rise were warmer than today (27°–29°C) (Norris et al., 2002; Forster et al., 2007). Oxygen isotope values of benthic foraminifers indicate a severe warming or a decrease in salinity of bottom waters at Demerara Rise at the base of OAE 2 (Friedrich et al., 2006). Rapid warming of SSTs was also suggested by Forster et al. (2007), who, on the basis of oxygen isotope values of planktonic foraminifers and TEX_{86} biomarker data, observed a rise of 6°C (to 35°–36°C) at the base of the OAE, paralleling the initial increase of carbon isotopes of OAE 2. SSTs drop shortly and for <150 k.y. after the initial warming to values lower than the pre-OAE conditions, reflecting the drawdown of atmospheric carbon dioxide, probably related to the intensive carbon burial during OAE 2 (Forster et al., 2007). Above this cooling interval, temperatures rise again, suggesting that circumstances leading to OAE 2 were stronger than the short-term storage capability of CO_2. Following OAE 2, SSTs remain in the thirties (Wilson et al., 2002; Forster et al., 2007). Positive carbon isotope values, high total organic carbon (TOC) contents, elevated Fe/Al and Co/Al ratios, and a lack of benthic foraminifers indicate severe anoxia, sometimes even euxinia, and an increase of surface water productivity during OAE 2 (Erbacher et al., 2005; Hetzel et al., 2006; Friedrich et al., 2006).

F6. $\delta^{13}C_{org}$ record showing OAE 2, p. 21.

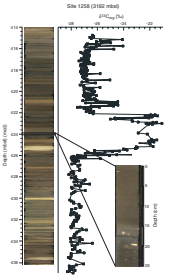

Late Cretaceous

SSTs remain warm following OAE 2 and throughout the Turonian (Forster et al., 2007; Bornemann and Norris, in press), whereas benthic oxygen isotope values indicate relatively fast cooling or an increase of bottom water salinity (Friedrich et al., 2006). A gradual SST decrease occurred in the latest Turonian and Coniacian with some short-term cooling events, which might be related to the buildup of ice shields at high latitudes (Bornemann and Norris, in press).

Black shale sedimentation at Demerara Rise ceased in the early Campanian. Based on benthic foraminiferal faunas, Friedrich and Erbacher (2006) suggested bottom water reoxygenated gradually during the late Santonian at the shallower parts of the Demerara Rise depth transect, whereas the deep end of the transect remained anoxic until the early Campanian. These authors proposed that this gradual ventilation from shallow to deep environments was related to the ongoing opening of the equatorial Atlantic Gateway.

Upper Campanian–Maastrichtian strata are represented by >200 m of chalk and calcareous claystones. Based on calcareous nannofossil assemblages, Thibault and Gardin (2006) described two cooling events during the Maastrichtian. A severe warming event in the latest Maastrichtian resulted in a decrease of surface water productivity prior to the K/P boundary. Stable carbon isotope studies of this latest Maastrichtian

interval likely were compromised by a diagenetic overprint (**MacLeod,** this volume, and discussion below).

Black Shales As Active Bioreactors

Forster et al. (2004), Meyers et al. (2006), and **Meyers and Bernasconi** (this volume) showed that Cenomanian–Santonian black shale sequences of Unit IV contain between 2 and 15 wt% organic carbon. High Rock-Eval hydrogen index (HI) values, low T_{max} values, and sterane and hopane biomarkers indicate that the bulk of organic matter is marine in origin and thermally immature. These authors determined that this organic matter is derived from mostly marine algal and microbial sources. Although $\delta^{13}C_{org}$ values and TOC/TN ratios mimic those of land-plant organic matter, contributions from land plants are considered minor. Elevated C/N ratios suggest depressed organic matter degradation, most likely associated with low-oxygen conditions in the water column that favored preservation of nitrogen-poor forms of organic matter over nitrogen-rich components. $\delta^{15}N_{total}$ values of the black shales fall between –4‰ and +1‰, which is much lower than modern ocean values of approximately +5‰. The low $\delta^{15}N$ values indicate that greatly amplified microbial nitrogen fixation accompanied black shale deposition and imply existence of strong near-surface stratification of the ocean.

During Leg 207, a high-resolution interstitial water sampling program was conducted to understand the impact of relatively deep seated organic matter–rich black shale sequences on diagenetic processes. Initial shipboard results suggested that the Cretaceous black shales are still active biogeochemically despite deposition >100 m.y. ago (Erbacher, Mosher, Malone, et al., 2004; Erbacher et al., 2004) (Fig. **F7**). Arndt et al. (2006) used an interstitial water transport-reaction model to characterize dominant biogeochemical processes operating in Demerara Rise sediments. Their results clearly indicate a single stratigraphic biogeochemical source and sink, the Cretaceous black shales, coupled with simple diffusion to and from the sediment/water interface, drives the entire biogeochemical system. Two processes dominate the system: organic matter degradation by methanogenesis within the shales and anaerobic methane oxidation (AMO) in the overlying sediments. Consumption of upward-diffusing methane and downward-diffusing sulfate during AMO drives an enhanced diffusional sulfate flux, producing linear profiles (Fig. **F7**). Deviations of linear sulfate gradients are the result of local porosity variability. Consumption of sulfate promotes remobilization of biogenic barium and precipitation of barite in the zone of oversaturation in the overlying sediments where sulfate content increases. Temporal shifts in the barite precipitation zone inhibited formation of barite fronts (Brumsack, 2006). Calculated methanogenic and AMO rates are much lower than reaction rates from shallow nearshore marine sediments but compare with the lower range of rate studies from other deep-marine sedimentary sections.

Meyers et al. (2004) suggested that it is likely that methane generation within the black shale units stemmed from in situ microbial activity because of the low thermal maturity of the organic carbon and the weak correspondence of higher TOC concentration and greater methane concentration. Attempts to quantify the microbial population were challenging despite these conclusions and the fact that interstitial water geochemistry clearly indicates an active biosphere. **Schippers and Neretin** (this volume) utilized direct microscopic counts using acridine

F7. Interstitial water sulfate, ammonium, barium, and methane, p. 22.

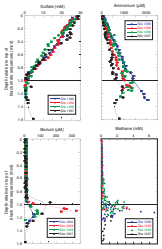

orange stain (AODC) and ribosomal ribonucleic acid (rRNA) techniques, specifically, catalyzed reporter deposition–fluorescence in situ hybridization (CARD-FISH), to investigate the microbial population within the black shales. Prokaryotes were detected in 2 of 13 black shale samples using both techniques, with total numbers comparable to sediments from previous studies of ODP cores. A few living cells of archaea were detected, but their numbers were too low to quantify using CARD-FISH. The absence of prokaryotes in most samples suggests that the black shales do not support a thriving microbial community. However, the presence of prokaryotes in high numbers in two samples indicates at least a patchy distribution of archaea, perhaps enough to catalyze the lower rates of reduction suggested by interstitial water studies. **Fredricks and Hinrichs** (this volume) analyzed black shales and overlying organic-lean sediments for the presence of intact polar lipids (IPL), which constitute the cell membranes of living microorganisms. Results document the presence of IPL in the organic-lean sediments, which likely are related to methane oxidation. IPL were difficult to detect in black shales, which was interpreted to be the result of the poor signal-to-noise ratio (low cell content in a high organic matter matrix). Initial studies of Demerara Rise sedimentary microbial populations suggest low microbial activity; however, cell distribution may be patchy in the black shales. Adequate substrate exists in the black shales to maintain an active biogeochemical system to dominate the interstitial water geochemical profiles.

Clayton et al. (this volume) measured iron isotopes in 10 black shale samples from Hole 1260B to gain a better understanding of oceanic redox during the mid-Cretaceous. Three extraction procedures separated Fe components in the sediments, which is a little-used technique for marine sediments. However, technical problems limited the scope of the planned work. δ^{56}Fe values of Fe oxide-sulfide-carbonate extracts range between 0.02‰ and –0.77‰ and negatively correlate to C/N ratios. In contrast, δ^{56}Fe values of two Fe oxide extracts are more positive (0.74‰ and 0.63‰), suggesting measurable fractionation within different Fe components in the cores. These results demonstrate the potential for selective extraction procedures to study fractionation of Fe isotopes and redox recycling is marine sediments.

Cretaceous/Paleogene Boundary

At three sites along the Demerara Rise depth transect (1258, 1259, and 1260) excellent examples of the K/P boundary were recovered, marked by a 2-cm-thick graded spherule layer at each site (Fig. **F8**). At a paleodistance of ~4500 km from the proposed Chicxulub meteorite impact crater, the K/P boundary succession at Demerara Rise is remarkably complete, and fine details of the sedimentological and paleontological expression of the event are recorded. These details include a record of seafloor sediment resuspension within minutes of the impact followed by deposition of a primary air fall over subsequent hours to weeks and a well-resolved record of the recovery and radiation of foraminifers over the first few million years (MacLeod et al., 2007) (Fig. **F8**). Faunal turnover at this boundary is dramatic. Sections near this interval include the uppermost Maastrichtian, a relatively extended P0 planktonic foraminiferal zone, and a complete succession of the lowermost Paleogene planktonic foraminiferal zones (MacLeod et al., 2007). Iridium concentrations reach a maximum of ~1.5 ppb at the top of the spherule bed; Ir

F8. K/P boundary concentrations of Ir, Co, Cr, and Ni, p. 23.

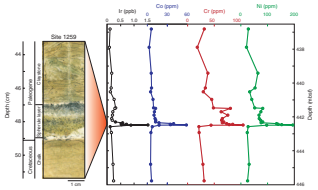

concentrations are otherwise below detection limits elsewhere in the core (MacLeod et al., 2007) (Fig. F8).

Paleogene Paleoceanography and the PETM

The PETM is an interval of extreme and abrupt global warming. All five of the Leg 207 sites recovered the Paleocene/Eocene boundary along a transect of 1300 m present water depth. With a thickness of ~2.5 m, the most expanded PETM interval at Demerara Rise was recovered at Site 1258 (Nuñes and Norris, 2006; Sexton et al., 2006) (Fig. F9). Low carbon isotope values (Fig. F9), however, argue for secondary geochemical overprinting of foraminifers. Calcareous nannofossils reacted with the appearance of classic "excursion taxa" during the PETM, which, in the case of Demerara Rise, parallel a sudden occurrence of malformed and eutrophic species. The latter are interpreted to be related to increased runoff with subsequent fertilization of the ocean off South America (Jiang and Wise, 2006). Ongoing high-resolution studies focusing on the inorganic geochemistry and nannofossil ecology of the PETM will contribute additional information about temperature excursions and their consequences during this event.

Eocene chalks, particularly through the lower–middle Eocene, are nearly continuous and expanded (~200 m thick) at Sites 1258 and 1260. Detailed stratigraphic studies based on calcareous nannofossils (Lupi and Wise, 2006) and paleomagnetism (**Suganuma and Ogg,** this volume) will serve as the basis for further high-resolution paleoceanographic and cyclostratigraphic studies. Sexton et al. (2006) present the first high-resolution benthic foraminiferal $\delta^{13}C$ and $\delta^{18}O$ records derived at one locality and not representing a composite from numerous sites (Fig. F10). In revealing a temporary warming period punctuating general middle Eocene cooling, data from Sexton et al. (2006) support the validity of the Eocene composite from Zachos et al. (2001). Sexton et al.'s (2006) $\delta^{13}C$ record suggests minimal interocean $\delta^{13}C$ gradients during the warm early and middle Eocene due either to a lack of deep-water sources derived from high latitudes or a reduction in the efficiency of the biological pump during these warm periods. Several intervals in Sexton et al.'s (2006) stable isotope record seem to indicate previously unknown short-lived warming events (e.g., at 52.6, 50.5, and 40.3 Ma).

Late Miocene Erosional Event

Broadly, the entire Cenozoic succession thickens inboard toward the shelf, where it is nearly 400 m thick at Site 1259, for example. Within this succession Neogene stratigraphy is distinctly separated from the Paleogene by a regional lower upper Miocene (Zone NN11a) unconformity that is clearly identifiable in seismic profile (Reflector A in Fig. F11) and in recovered cores (Ingram and Wise, 2006). **O'Regan and Moran** (this volume) estimate in excess of 220 m of sediment removal during this erosional event. In addition, evidence of ongoing faulting through the section and widespread sediment failure immediately above this unconformity resulted in a slump deposit observed at Site 1261 (Zone NN11b) (Ingram and Wise, 2006).

It is possible that strong currents swept across the rise, eroding Miocene and older sediments. Expansion of Antarctic ice sheets during the middle to late Miocene influenced bottom water formation and upwelling along Atlantic continental margins. Concurrently, the Central

F9. $\delta^{13}C$ record at Site 1258 through the PETM, p. 24.

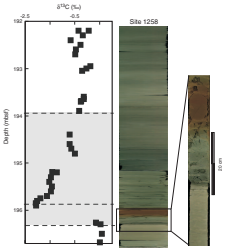

F10. $\delta^{13}C$ and $\delta^{18}O$ records compared with multisite compilations, p. 25.

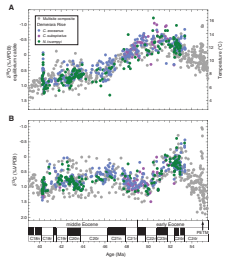

F11. Seismic section showing the A horizon near Site 1261, p. 26.

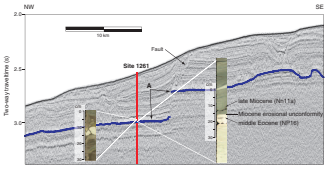

American Seaway (CAS) shoaled, preventing deepwater exchange between the Pacific and Atlantic Oceans (Nisancioglu et al., 2003). These broad-scale changes in ocean circulation may have been responsible for generating currents that swept across outer Demerara Rise, causing the late Miocene unconformity. Alternatively, the close proximity of the slump identified at Site 1261 with faulting shown in seismic profiles indicates a relationship between possible late-stage tectonic activity and this mass failure deposit. Ingram and Wise (2006) believe that a single mass failure event may have been responsible for late Miocene erosion and creation of the A reflection horizon as shown in Figure **F11.**

Chronostratigraphy

Critical to further paleoceanographic investigations is the establishment of an accurate chronostratigraphic framework and recognition of hiatuses for the stratigraphic sections investigated. **MacLeod** (this volume), for example, points out the difficulty in correlating site to site results, given the present understanding of age control. Although not yet developed, robust chronostratigraphy will come about through contributions pertaining to integration of site results (e.g., modified composite depth scales) and establishment of time marker horizons and cyclostratigraphic tuning. For example, **Suganuma and Ogg** (this volume) identified paleomagnetic polarity Chrons C18n–C27r of middle Eocene to late Paleocene age and Chrons C29r through potentially C34n of Maastrichtian–Campanian age. Erbacher et al. (2005) established the position of the Cenomanian/Turonian boundary interval and position of OAE 2 from $\delta^{13}C$ measurements, with this being a critical time horizon that provides a base for subsequent paleoceanographic studies on upper Cenomanian to lower Turonian sediments. **O'Regan** (this volume) established an equivalent log depth scale of the Cretaceous section by tying core depths to logging depths using curve matching of physical property data. This improved depth scale will permit cyclostratigraphic analysis and orbital tuning to further refine age control, such as the work of **Nederbragt et al.** (this volume). Ingram and Wise (2006) studied nannofossils of Cenozoic sections to establish the age stratigraphy and recognize a number of hiatuses and used $\delta^{18}O$ and $\delta^{13}C$ to establish the Oligocene/Eocene boundary.

SUMMARY

Early scientific results from Leg 207 on Demerara Rise document some fundamental discoveries. As examples, seismic sections from the site survey data document South America/Africa continental breakapart in the Early Cretaceous, allowing linkage of the southern and northern Atlantic Oceans. This break-apart is rapidly followed by onset of broad-scale and long-lasting ocean anoxia, as shown by deposition of upper Albian to Santonian organic-rich black shale sediments (Myers et al., 2004, 2006; **Meyers and Bernasconi,** this volume). Organic and inorganic geochemistry results show the importance of these black shale sediments in driving the geochemistry of the entire sediment section through methanogenesis (e.g., Arndt et al., 2006). A surprising observation, however, is the discovery of few microbial organisms inhabiting the sediments of the black shale sequences, although their presence is expected to be patchy in distribution (**Schippers and Neretin,** this volume; **Fredricks and Hinrichs,** this volume). Important understanding

of hydrocarbon source rocks (e.g., Meyers et al., 2006) and the Cretaceous paleoceanographic and atmospheric conditions that created them are gained through these investigations (e.g., Bice et al., 2006).

Critical intervals of rapid paleoceanographic change were successfully sampled and studied following completion of Leg 207. Ocean anoxic events, such as OAE 1d, the MCE, and OAE 2 correlate with examples around the world and provide significant detail about climate and/or circulation changes through recovery of relatively expanded sedimentary sections (e.g., Kulhanek and Wise, 2006; Friedrich et al., 2006; Erbacher et al., 2005). Erbacher et al. (2005), for example, present the first high-resolution carbon isotope records across OAE 2 from the South American margin of the tropical Atlantic. Recovery of the first well-preserved and detailed records of the K/P impact event off the South American coast were recovered during Leg 207 (e.g., MacLeod et al., 2007), documenting the sequence of fall out and faunal turnover as a result of the meteorite impact ~4500 km distant. Excellent expanded records of the PETM were also recovered during Leg 207. Nuñes and Norris (2006) show rapid ocean temperature changes, faunal turnover, and an abrupt reversal in ocean overturning using data from Leg 207 samples. Sexton et al. (2006) present the first high-resolution benthic foraminiferal $\delta^{13}C$ and $\delta^{18}O$ records derived at one locality (i.e., not a composite from several sites), revealing temporary warming punctuating general middle Eocene cooling. Their data also seem to indicate additional previously unknown short-lived warming events (e.g., at 52.6, 50.5, and 40.3 Ma). As a final example, Ingram and Wise (2006) interpret large-scale mass failure in the late Miocene from hiatus stratigraphy, potentially tectonically triggered or related to massive gas hydrate dissociation due to paleoceanographic changes. Extensive erosion on Demerara Rise at this time may be related to expanding ice sheets and closure of the Isthmus of Panama, causing marked changes in global ocean circulation patterns.

ACKNOWLEDGMENTS

The authors would like to thank in particular the officers and crew of the *JOIDES Resolution* and the Ocean Drilling Program staff, Leg 207. The studies included within this volume and beyond would not have been possible without their outstanding support. We would also like to thank all the participating scientists, both those who sailed with us and the shore-based contributors. They've been a terrific team to work with on board ship and off, and we appreciate their enthusiasm in sharing results with us. We would like to express our limitless appreciation to Drs. V. Speiss and L. Zuelsdorff of the University of Bremen for acquiring and processing the site survey seismic data and H. Meyer of BGR for reprocessing the industry MCS data. All these seismic data were made readily available for our research. We also wish to express our gratitude to our respective institutions (Natural Resources Canada, Bundesanstalt für Geowissenschaften und Rohstoffe, and the Ocean Drilling Program) for supporting each of us in these studies. Critical reviews of this manuscript by Drs. D.J. Thomas and L.J. Clarke are greatly appreciated. This research used samples and data provided by the Ocean Drilling Program (ODP). ODP was funded by the U.S. National Science Foundation (NSF) and participating countries under management of Joint Oceanographic Institutions (JOI), Inc. Natural Resources Canada ESS contribution number 20060664.

REFERENCES

Arndt, S., Brumsack, H.-J., and Wirtz, K.W., 2006. Cretaceous black shales as active bioreactors: a biogeochemical model for the deep biosphere encountered during ODP Leg 207 (Demerara rise). *Geochim. Cosmochim. Acta,* 70(2):408–425. **doi:10.1016/j.gca.2005.09.010**

Benkhelil, J., Mascle, J., and Tricart, P., 1995. The Guinea continental margin: an example of a structurally complex transform margin. *Tectonophysics,* 248(1–2):117–137. **doi:10.1016/0040-1951(94)00246-6**

Bice, K.L., Birgel, D., Meyers, P.A., Dahl, K.A., Hinrichs, K.-U., and Norris, R.D., 2006. A multiple proxy and model study of Cretaceous upper ocean temperatures and atmospheric CO_2 concentrations. *Paleoceanography,* 21(2):PA2002. **doi:10.1029/2005PA001203**

Bornemann, A., and Norris, R.D., in press. Planktic foraminifer photosymbiosis, depth habitats and super-warm tropics during the Cretaceous thermal maximum. *Mar. Micropaleontol.*

Brumsack, H.-J., 2006. The trace metal content of recent organic carbon-rich sediments: implications for Cretaceous black shale formation. *Palaeogeogr., Palaeoclimatol., Palaeoecol.,* 232(2–4):344–361. **doi:10.1016/j.palaeo.2005.05.011**

Coxall, H.K., D'Hondt, S., and Zachos, J.C., 2006. Pelagic evolution and environmental recovery after the Cretaceous–Paleogene mass extinction. *Geology,* 34(4):297–300. **doi:10.1130/G21702.1**

Erbacher, J., Friedrich, O., Wilson, P.A., Birch, H., and Mutterlose, J., 2005. Stable organic carbon isotope stratigraphy across oceanic anoxic Event 2 of Demerara rise, western tropical Atlantic. *Geochem., Geophys., Geosyst.,* 6(6):Q06010. **doi:10.1029/2004GC000850**

Erbacher, J., Huber, B.T., and Norris, R., 2003. The suffocation of an ocean. *In* White, K., and Urquhart, E. (Eds.), *ODP Highlights:* Washington, D.C. (Joint Oceanographic Institutes), 12–13.

Erbacher, J., Mosher, D.C., and Malone, M.J., 2004. Drilling probes past carbon cycle perturbations on Demerara rise. *Eos, Trans. Am. Geophys. Union,* 85(6):57–63. **doi:10.1029/2004EO060001**

Erbacher, J., Mosher, D.C., Malone, M.J., et al., 2004. *Proc. ODP, Init. Repts.,* 207: College Station, TX (Ocean Drilling Program). **doi:10.2973/odp.proc.ir.207.2004**

Flicoteaux, R., Latil-Brun, M.-V., and Michaud, L., 1988. Histoire de la subsidence post-rift du bassin côtier mauritano-sénégalo-guinéen. Relation avec l'amincissement crustal pendant la période jurassique à Crétacé inférieur. Comparaison avec l'évolution des marges péri-atlantiques au niveau de l'Atlantique central et equatorial (côte est des U.S.A., Sud-Sahara, Côte d'Ivoire et Plateau du Demerara). *In* Sougy, J., and Rodgers, J. (Eds.), *The West African Connection: Evolution of the Central Atlantic Ocean and its Continental Margins.* J. Afr. Earth Sci., 7(2):345–359. **doi:10.1016/0899-5362(88)90079-6**

Friedrich, O., and Erbacher, J., 2006. Benthic foraminiferal assemblages from Demerara Rise (ODP Leg 207, western tropical Atlantic): possible evidence for a progressive opening of the equatorial Atlantic gateway. *Cretaceous Res.,* 27(3):377–397. **doi:10.1016/j.cretres.2005.07.006**

Friedrich, O., Erbacher, J., and Mutterlose, J., 2006. Paleoenvironmental changes across the Cenomanian/Turonian boundary event (oceanic anoxic Event 2) as indicated by benthic foraminifera from the Demerara Rise (ODP Leg 207). *In* Erbacher, J., Danelian, T., and Nishi, H. (Eds.), *Demerara Rise (Leg 207): Equatorial Cretaceous and Palaeogene Stratigraphy and Paleoceanography, Part I.* Rev. Micropaleontol., 49(3):121–139. **doi:10.1016/j.revmic.2006.04.003**

Forster, A., Schouten, S., Moriya, K., Wilson, P.A., and Sinninghe Damsté, J.S., 2007. Tropical warming and intermittent cooling during the Cenomanian/Turonian oce-

anic anoxic Event 2: sea surface temperature records from the equatorial Atlantic. *Paleoceanography,* 22:PA1219. **doi:10.1029/2006PA001349**

Forster, A., Sturt, H., Meyers, P.A., and Shipboard Scientific Party, 2004. Molecular biogeochemistry of Cretaceous black shales from the Demerara Rise: preliminary shipboard results from Sites 1257 and 1258, Leg 207. *In* Erbacher, J., Mosher, D.C., Malone, M.J., et al., *Proc. ODP, Init. Repts.,* 207: College Station, TX (Ocean Drilling Program), 1–22. **doi:10.2973/odp.proc.ir.207.110.2004**

Gouyet, S., Unternehr, P., and Mascle, A., 1994. The French Guyana margin and the Demerara Plateau: geologic history and petroleum plays. *In* Mascle, A. (Ed.), *Hydrocarbon and Petroleum Geology of France*. Spec. Publ.—Eur. Assoc. Pet. Geosci., 4:411–422.

Haq, B.U., Hardenbol, J., and Vail, P.R., 1988. Mesozoic and Cenozoic chronostratigraphy and cycles of sea-level change. *In* Wilgus, C.K., Hastings, B.S., Kendall, C.G. St.C., Posamentier, H.W., Ross, C.A., and Van Wagoner, J.C. (Eds.), *Sea-Level Changes—An Integrated Approach*. Spec. Publ.—SEPM, 42:72–108.

Hardas, P., and Mutterlose, J., 2006. Calcareous nannofossil biostratigraphy of the Cenomanian/Turonian boundary interval of ODP Leg 207 at the Demerara Rise. *In* Erbacher, J., Danelian, T., and Nishi, H. (Eds.), *Demerara Rise (Leg 207): Equatorial Cretaceous and Palaeogene Stratigraphy and Paleoceanography, Part I*. Rev. Micropaleontol., 49(3):165–179. **doi:10.1016/j.revmic.2006.04.005**

Hayes, D.E., Pimm, A.C., et al., 1972. *Init. Repts. DSDP,* 14: Washington (U.S. Govt. Printing Office).

Hetzel, A., Forster, A., and Brumsack, H.-J., 2006. Depositional environment of Cenomanian/Turonian black shales from Demerara Rise (ODP Leg 207)—implications from trace metal patterns. *Geophys. Res. Abstr.,* 8:09360.

Ingram, W.C., and Wise, S.W., 2006. Anatomy of Oligocene–Miocene debris flows and slumps from Demerara Rise: implications for margin destruction [American Association of Petroleum Geologists 2006 Annual Convention, Houston, 11–14 April 2006]. (Abstract)

Jiang, S., and Wise, Jr., S.W., 2006. Surface-water chemistry and fertility variations in the tropical Atlantic across the Paleocene/Eocene Thermal Maximum as evidenced by calcareous nannoplankton from ODP Leg 207, Hole 1259B. *In* Erbacher, J., Danelian, T., and Nishi, H. (Eds.), *Demerara Rise (Leg 207): Equatorial Cretaceous and Palaeogene Stratigraphy and Paleoceanography, Part II*. Rev. Micropaleontol., 49(4):227–244. **doi:10.1016/j.revmic.2006.10.002**

Kulhanek, D.K., and Wise, Jr., S.W., 2006. Albian calcareous nannofossils from ODP Site 1258, Demerara Rise. *In* Erbacher, J., Danelian, T., and Nishi, H. (Eds.), *Demerara Rise (Leg 207): Equatorial Cretaceous and Palaeogene Stratigraphy and Paleoceanography, Part I*. Rev. Micropaleontol., 49(3):181–195. **doi:10.1016/j.revmic.2006.06.002**

Lupi, C., and Wise, Jr., S.W., 2006. Calcareous nannofossil biostratigraphic framework for middle Eocene sediments from ODP Hole 1260A, Demerara Rise. *In* Erbacher, J., Danelian, T., and Nishi, H. (Eds.), *Demerara Rise (Leg 207): Equatorial Cretaceous and Palaeogene Stratigraphy and Paleoceanography, Part II*. Rev. Micropaleontol., 49(4):245–253. **doi:10.1016/j.revmic.2006.10.001**

MacLeod, K.G., Whitney, D.L., Huber, B.T., and Koeberl, C., 2007. Impact and extinction in remarkably complete K/T boundary sections from Demerara rise, tropical western North Atlantic. *GSA Bull.,* 119:101–115.

Meyers, P.A., Bernasconi, S.M., and Forster, A., 2006. Origins and accumulation of organic matter in expanded Albian to Santonian black shale sequences on the Demerara Rise, South American margin. *Org. Geochem.,* 37(12):1816–1830. **doi:10.1016/j.orggeochem.2006.08.009**

Meyers, P.A., Forster, A., Sturt, H., and Shipboard Scientific Party, 2004. Microbial gases in black shale sequences on the Demerara Rise. *In* Erbacher, J., Mosher, D.C., Malone, M.J., et al., *Proc. ODP, Init. Repts.,* 207: College Station, TX (Ocean Drilling Program), 1–18. **doi:10.2973/odp.proc.ir.207.109.2004**

Moriya, K., Wilson, P.A., Friedrich, O., Erbacher, J., and Kawahata, H., in press. Testing for ice sheets during the mid-Cretaceous greenhouse using glassy foraminiferal calcite from the mid-Cenomanian tropics on Demerara rise. *Geology*.

Nisancioglu, K.H., Raymo, M.E., and Stone, P.H., 2003. Reorganization of Miocene deep water circulation in response to the shoaling of the Central American Seaway. *Paleoceanography,* 18(1):1006. **doi:10.1029/2002PA000767**

Norris, R.D., Bice, K.L., Magno, E.A., and Wilson, P.A., 2002. Jiggling the tropical thermostat in the Cretaceous hothouse. *Geology,* 30(4):299–302. **doi:10.1130/0091-7613(2002)030<0299:JTTTIT>2.0.CO;2**

Nuñes, F., and Norris, R.D., 2006. Abrupt reversal in ocean overturning during the Palaeocene/Eocene warm period. *Nature (London, U. K.),* 439(7072):60–63. **doi:10.1038/nature04386**

Owen, H.G., and Mutterlose, J., 2006. Late Albian ammonites from offshore Suriname: implications for biostratigraphy and palaeobiogeography. *Cretaceous Res.,* 27(6):717–727. **doi:10.1016/j.cretres.2005.12.001**

Sexton, P.F., Wilson, P.A., and Norris, R.D., 2006. Testing the Cenozoic multisite composite $\delta^{18}O$ and $\delta^{13}C$ curves: new monospecific Eocene records from a single locality, Demerara Rise (Ocean Drilling Program Leg 207). *Paleoceanography,* 21(2):PA2019. **doi:10.1029/2005PA001253**

Thibault, N., and Gardin, S., 2006. Maastrichtian calcareous nannofossil biostratigraphy and paleoecology in the equatorial Atlantic (Demerara Rise, ODP Leg 207 Hole 1258A). *In* Erbacher, J., Danelian, T., and Nishi, H. (Eds.), *Demerara Rise (Leg 207): Equatorial Cretaceous and Palaeogene Stratigraphy and Paleoceanography, Part II*. Rev. Micropaleontol., 49(4):199–214. **doi:10.1016/j.revmic.2006.08.002**

Wilson, P.A., Norris, R.D., and Cooper, M.J., 2002. Testing the Cretaceous greenhouse hypothesis using glassy foraminiferal calcite from the core of Turonian tropics on Demerara Rise. *Geology,* 30(7):607–610. **doi:10.1130/0091-7613(2002)030<0607:TTCGHU>2.0.CO;2**

Zachos, J., Pagani, M., Sloan, L., Thomas, E., and Billups, K., 2001. Trends, rhythms, and aberrations in global climate 65 Ma to present. *Science,* 292(5517):686–693. **doi:10.1126/science.1059412**

Zachos, J.C., Schouten, S., Bohaty, S., Quattlebaum, T., Sluijs, A., Brinkhuis, H., Gibbs, S.J., and Bralower, T.J., 2006. Extreme warming of mid-latitude coastal ocean during the Paleocene–Eocene Thermal Maximum: inferences from TEX_{86} and isotope data. *Geology,* 34(9):737–740. **doi:10.1130/G22522.1**

Figure F1. Location map of outer Demerara Rise showing drill site locations and positions of seismic grid lines. Seismic lines used in subsequent figures are highlighted.

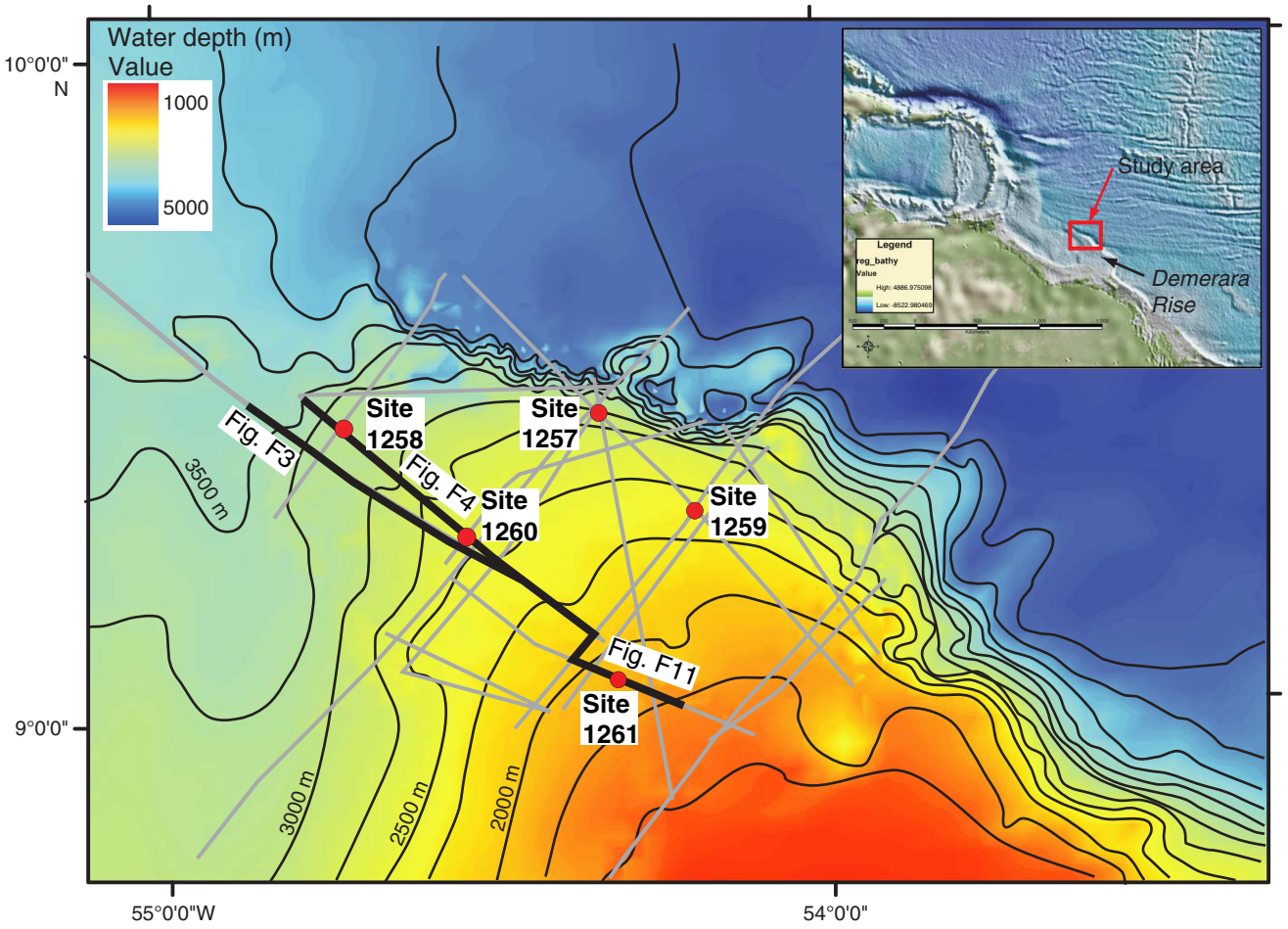

Figure F2. Morphologic map of the equatorial Atlantic showing the conjugate margins of Demerara Rise and Guinea Plateau, separated by the Guinea Fracture Zone.

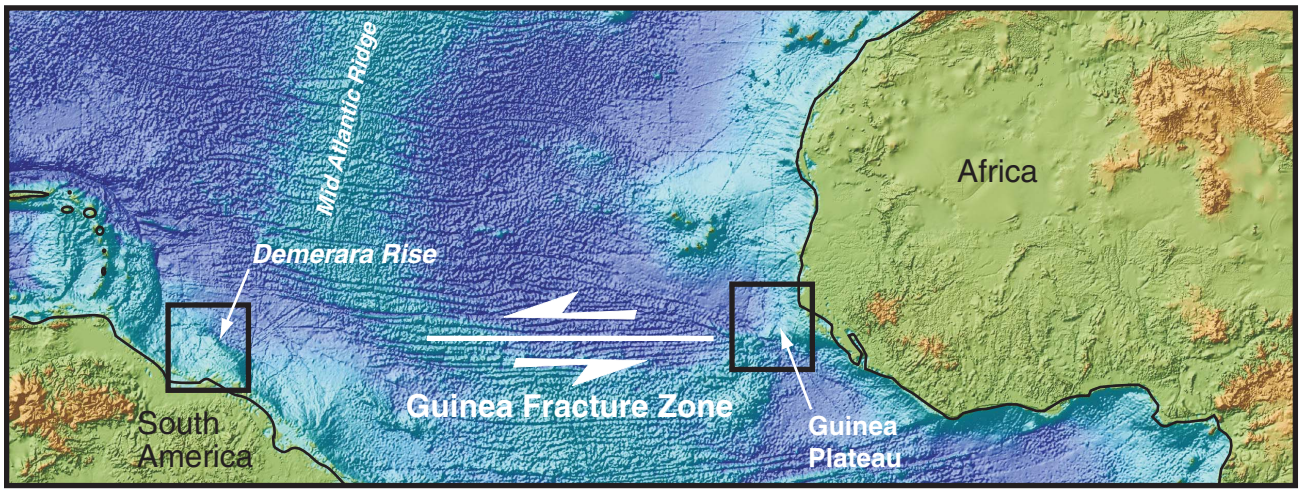

Figure F3. Industry multichannel seismic line (C2211) on the northern ramp of Demerara Rise, showing the prominent C reflector unconformity and the prominence and pattern of subsurface faulting (from Erbacher, Mosher, Malone, et al., 2004). The location of the seismic image shown in Figure F4, p. 19, is outlined.

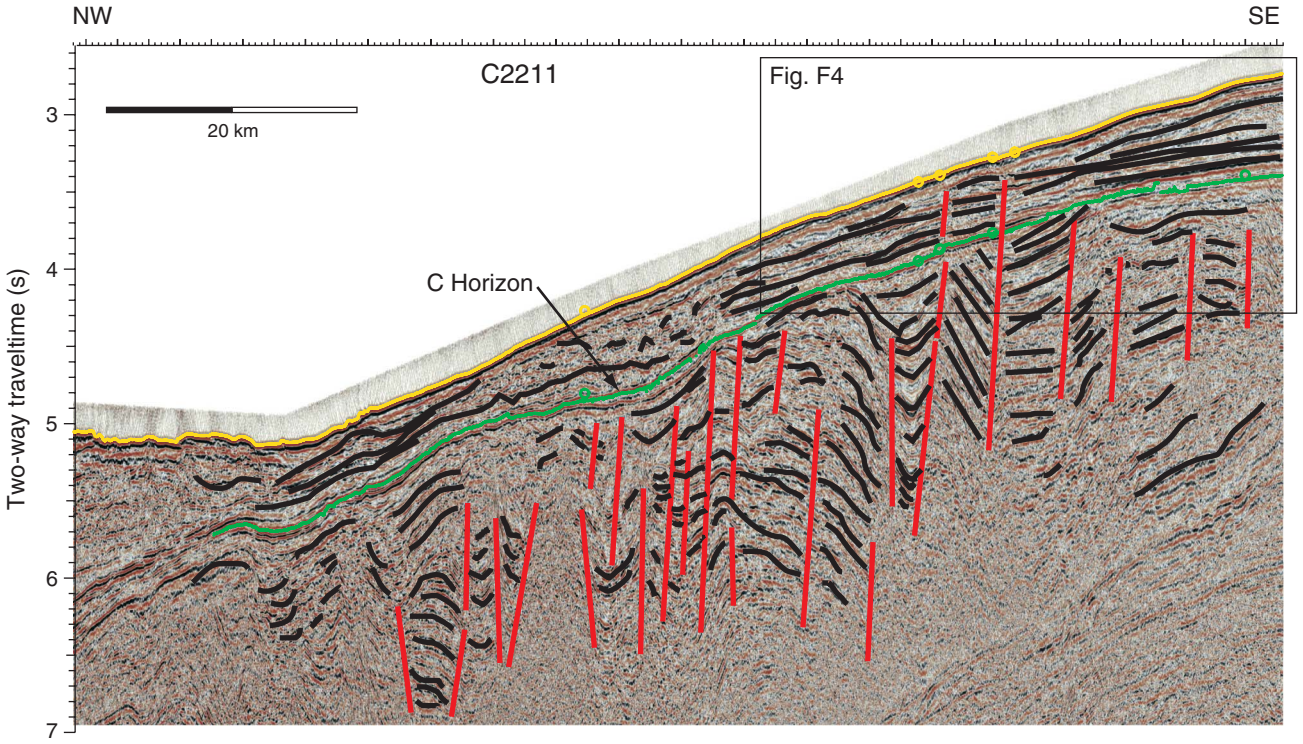

Figure F4. Composite image of site survey seismic reflection data through three Leg 207 drill sites (Lines GeoB213, GeoB214, and 207-L1S), showing seismic stratigraphy above the C reflection horizon.

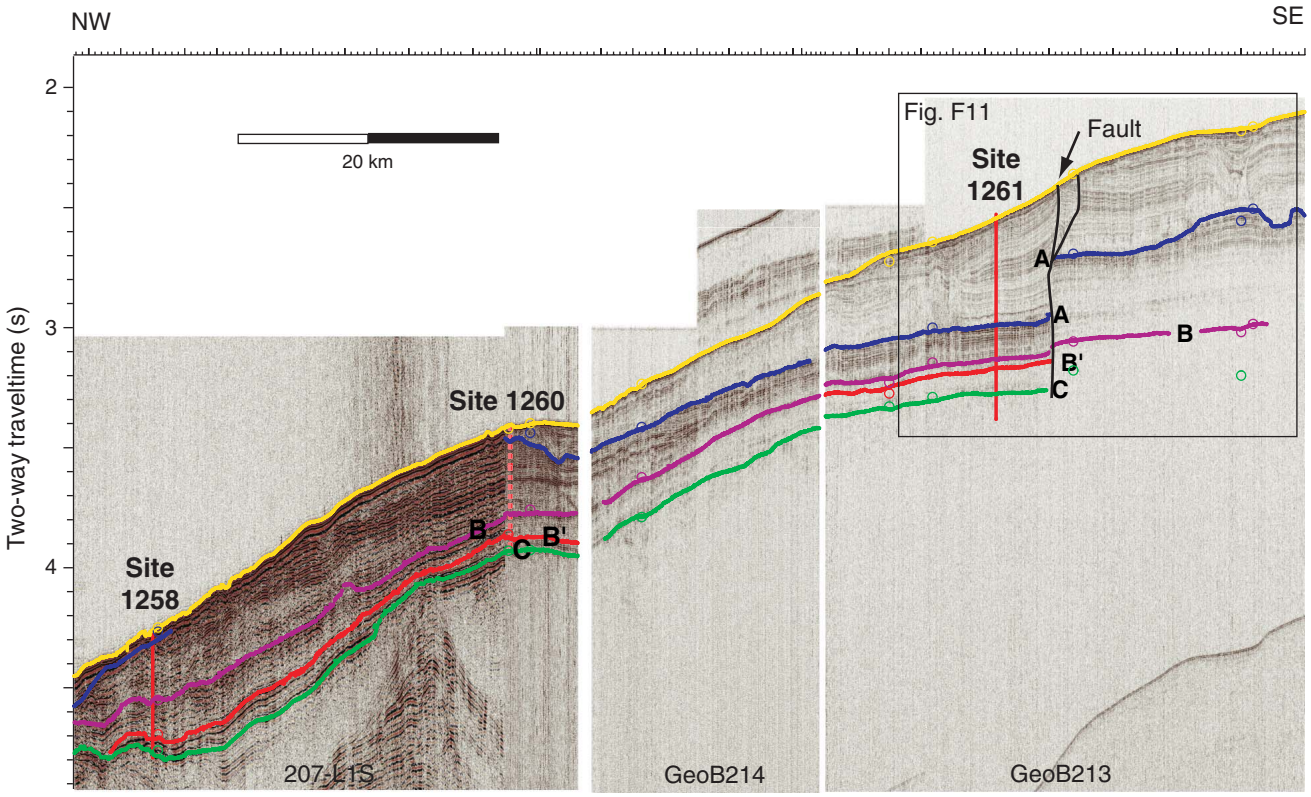

Figure F5. Example of the seismic to core correlation (Site 1259), as conducted with a synthetic seismogram (from Erbacher, Mosher, Malone, et al., 2004). The synthetic seismogram was generated using merged data from drill site check shot, logging, and core measured velocity and density data, convolved with an idealized Ormsby wavelet. No attempt was made at simulating multiple path reflections, nor amplitude preservation. Using sediment acoustic velocities derived from this correlation, the seismic data were migrated to the depth domain. Each site was correlated in a similar manner.

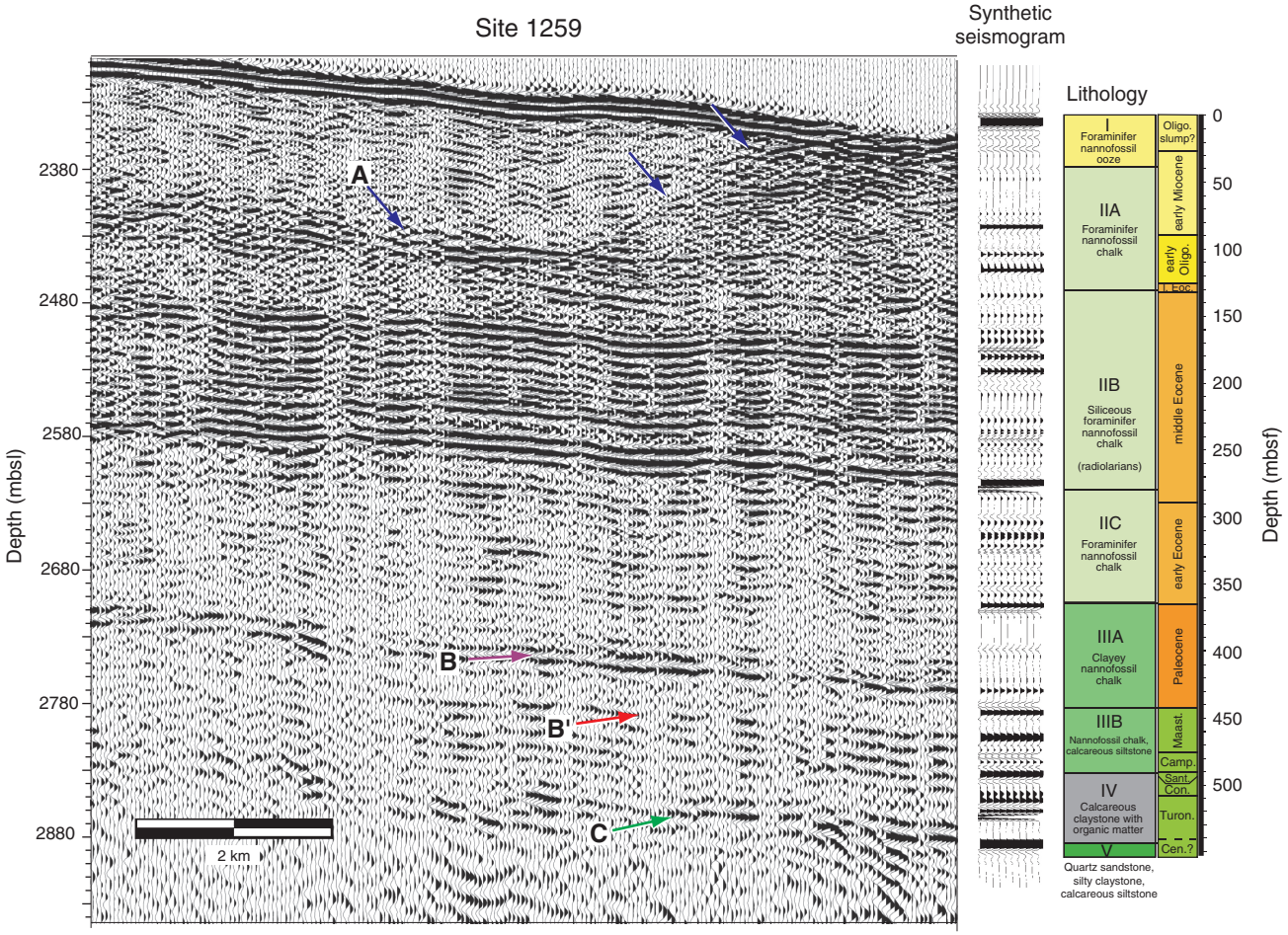

Figure F6. $\delta^{13}C_{org}$ record from Site 1258 showing the excursion considered to represent OAE 2 (after Erbacher et al., 2005). The adjacent photo is a highly vertically compressed photomosaic of recovered cores. Depths are in meters using the modified composite depth scale. The inset photo is a sample core image within OAE 2, displayed with the correct aspect ratio.

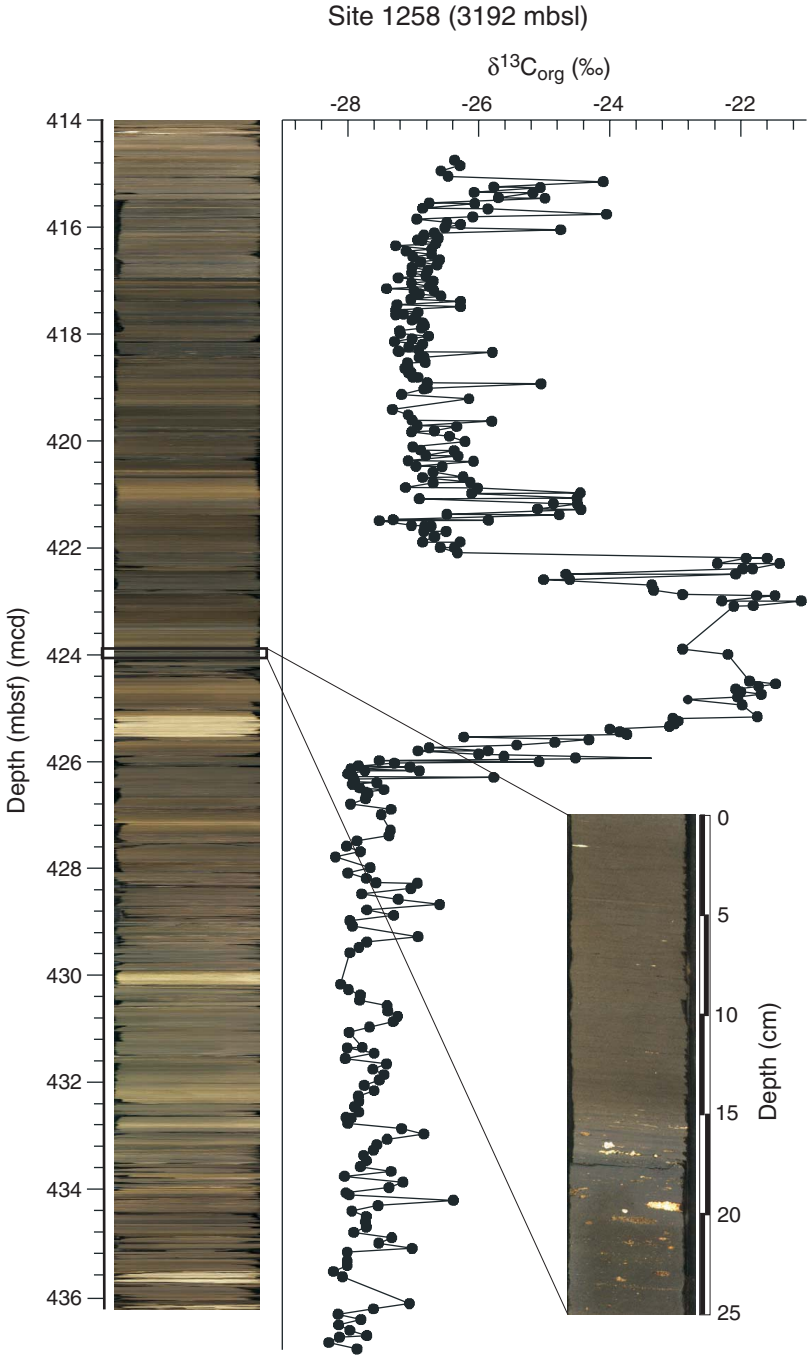

Figure F7. Measured interstitial water profiles of sulfate, ammonium, barium, and methane at four drilling sites (Sites 1257–1260, Demerara Rise) (after Erbacher, Mosher, Malone, et al., 2004; Arndt et al., 2006). The depth is given normalized to the top of the respective black shale sequence (assigned a value of 1 and represented by the horizontal solid black line in each diagram).

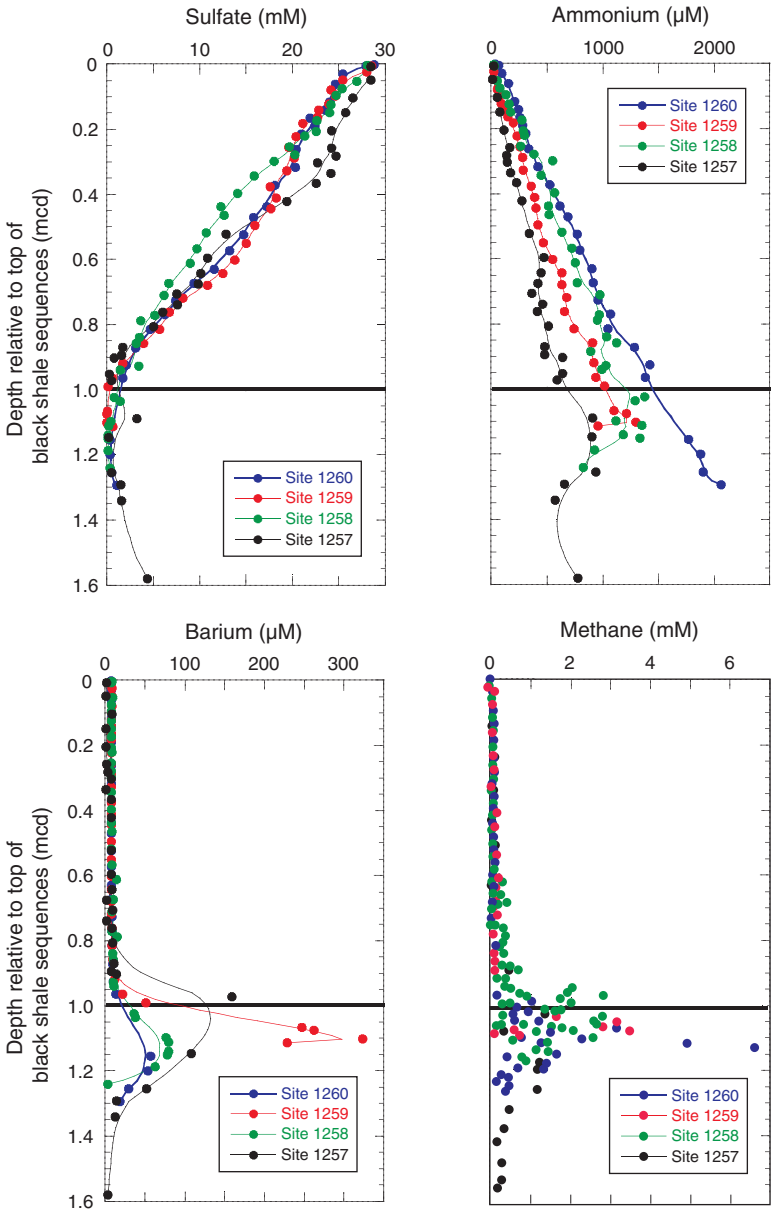

Figure F8. Cretaceous/Paleogene boundary concentrations of Ir, Co, Cr, and Ni through Section 207-1259C-8R-5 along with the core photo showing the spherule bed (after MacLeod et al., 2007). Ir concentrations in samples plotted as open circles were at or below detection limits, and the value plotted represents the calculated detection limit (i.e., the maximum concentration in these samples allowed by the analyses).

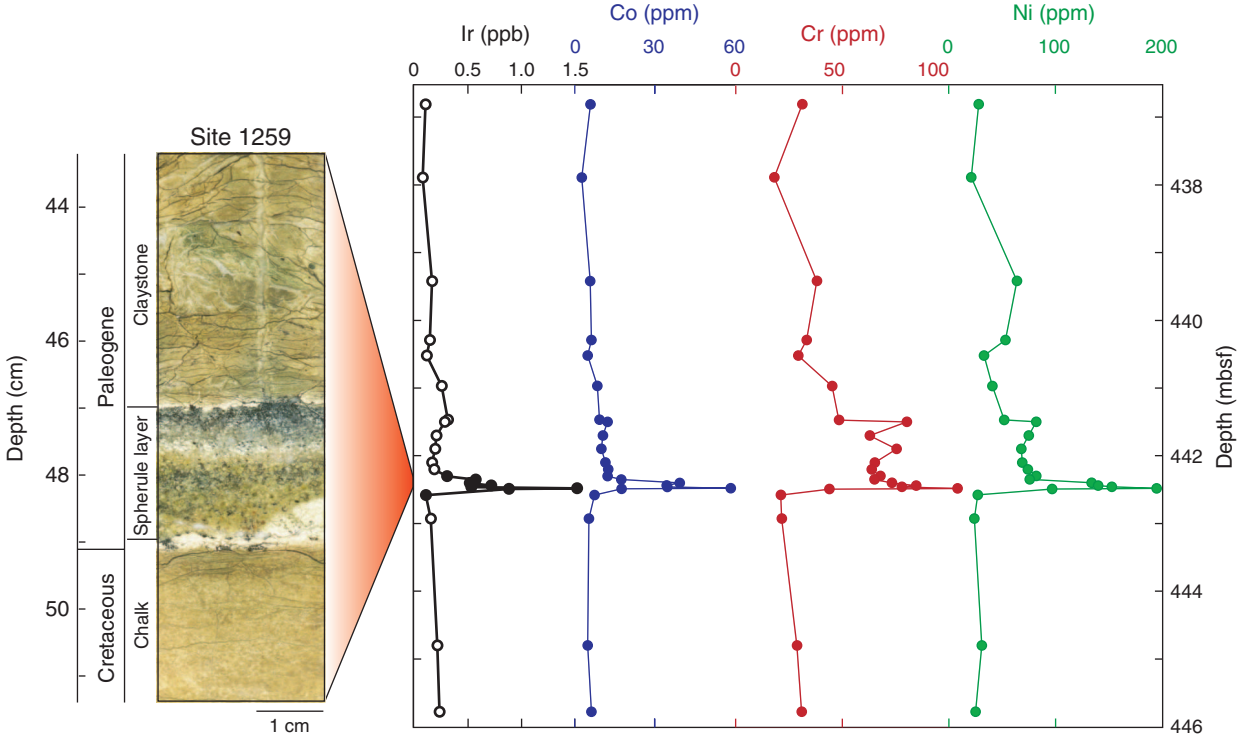

Figure F9. $\delta^{13}C$ record at Site 1258 through the Paleocene/Eocene Thermal Maximum (PETM) (after Nuñes and Norris, 2006). The adjacent core photo is highly vertically compressed. The inset core photo is of the boundary and is shown with the correct aspect ratio.

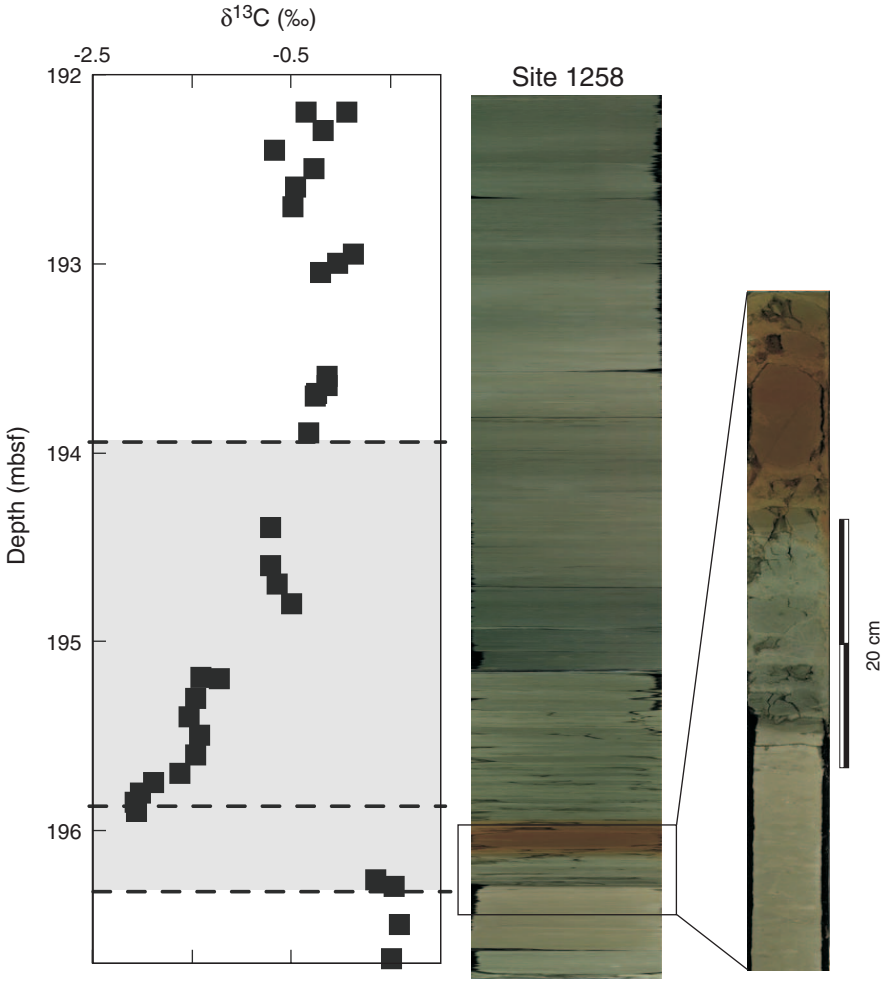

Figure F10. $\delta^{13}C$ and $\delta^{18}O$ records of analyses on single species through early and middle Eocene sections of cores from the Demerara Rise, compared with multisite compilations from other studies (see Sexton et al., 2006, for details). PETM = Paleocene/Eocene Thermal Maximum, VPDB = Vienna peedee belemnite.

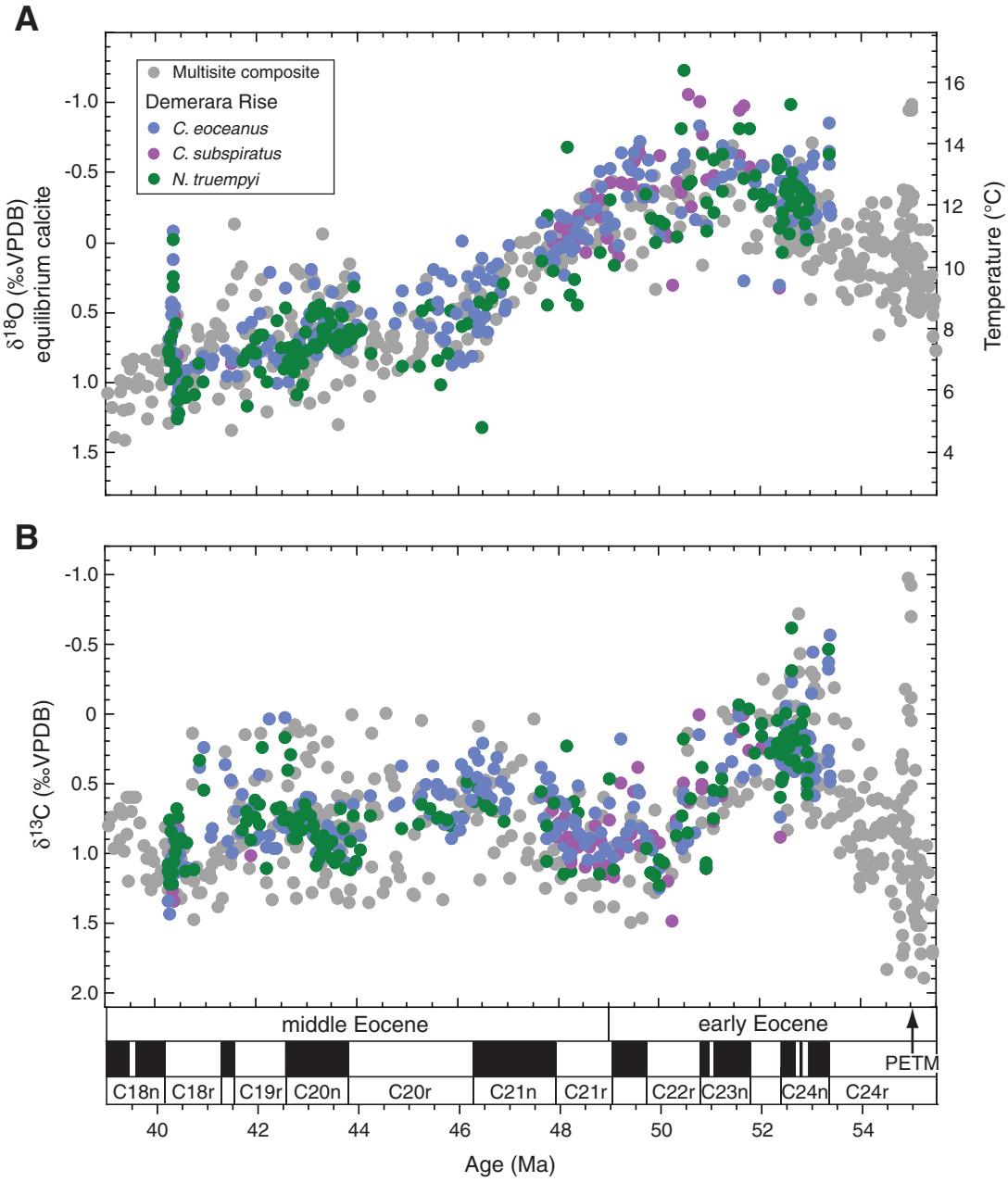

Figure F11. High-resolution seismic section (Line GeoB213) showing the A horizon near Site 1261. Insets of core photos show the slump zone overlying the Miocene erosional unconformity, determined by Ingram and Wise (2006) from nannofossil zonations as late Miocene in age.